

# Effect of H<sub>2</sub>O<sub>2</sub>/HCl Heat Treatment of Implants on In Vivo Peri-implant Bone Formation

Guo-li Yang, PhD, DDS<sup>1</sup>/Fu-ming He, PhD, DDS<sup>2</sup>/Shan-shan Zhao, BA<sup>3</sup>/  
Xiao-xiang Wang, DE<sup>4</sup>/Shi-fang Zhao, MD, DDS<sup>5</sup>

**Purpose:** To investigate the effect of H<sub>2</sub>O<sub>2</sub>/HCl heat treatment on peri-implant bone formation in vivo. **Materials and Methods:** Twenty Ti-6Al-4V implants and 30 Ti-6Al-4V discs were used in this study. The implants and discs were separated into 2 groups: sandblasted and dual acid-etched group (control group) and sandblasted, dual acid-etched and H<sub>2</sub>O<sub>2</sub>/HCl heat-treated group (test group). Surface morphology, roughness, and crystal structure of the discs were analyzed by field-emission scanning electron microscopy, atomic force microscopy, and low angle X-ray diffractometry. The implants were inserted into the femurs of 10 adult white rabbits. Animals were injected with fluorescent bone labels at 1, 5, and 7 weeks following surgery to monitor progress of bone formation. Animals were euthanized 8 weeks postsurgery, and block biopsies were prepared for histologic and histometric analysis. **Results:** Microscopic evaluation showed the surfaces were quite irregular for both techniques; however, the test surface demonstrated consistently smaller surface irregularities. The differences in Sa values were significant (P = .022). No significant differences were found in the maximum peak-to-valley ratio values (P = .258). X-ray diffractometry analysis showed that titanium dioxide was found on the test surface. New bone was formed on both implant surfaces. The bone-implant contact pattern appeared to produce a broad-based direct contact. Test implants demonstrated 7.13% more bone to implant contact (P = .003) and 15.42% more bone to implant contact for 3 consecutive threads (P = .001) than control implants. Test implants demonstrated 37.04% more bone area 500 μm outside of implant threads (P = .004) and 51.97% more bone area within 3 consecutive threads (P = .001) than control implants. No significant differences were found in bone area within all implant threads between the two groups (P = .069). **Conclusion:** This study demonstrated that implants heat-treated with H<sub>2</sub>O<sub>2</sub>/HCl solution enhanced peri-implant bone formation. INT J ORAL MAXILLOFAC IMPLANTS 2008;23:1020-1028.

**Key words:** H<sub>2</sub>O<sub>2</sub>/HCl heat treatment, osseointegration, surface morphology, surface roughness, titanium dioxide

<sup>1</sup>Resident Doctor, Department of Oral and Maxillofacial Surgery, Stomatology Hospital, School of Medicine, Zhejiang University, Yan'an Road, Hangzhou, China.

<sup>2</sup>Attending Doctor, Department of Prosthodontics, Stomatology Hospital, School of Medicine, Zhejiang University, Yan'an Road, Hangzhou, China.

<sup>3</sup>Resident Doctor, Department of Prosthodontics, Stomatology Hospital, School of Medicine, Zhejiang University, Yan'an Road, Hangzhou, China.

<sup>4</sup>Professor, Department of Materials Science and Engineering, Zhejiang University, Zheda Road, Hangzhou, China.

<sup>5</sup>Professor, Department of Oral and Maxillofacial Surgery, Stomatology Hospital, School of Medicine, Zhejiang University, Yan'an Road, Hangzhou, China.

**Correspondence to:** Professor Shi-fang Zhao, Department of Oral and Maxillofacial Surgery, Stomatology Hospital, School of Medicine, Zhejiang University, Yan'an Road, Hangzhou, 310006, China. E-mail: yangguoli123456@yahoo.com.cn

The endosseous dental implant has become a scientifically accepted and well-documented treatment for fully and partially edentulous patients.<sup>1-10</sup> Researchers indicated that the success of implants relied on condition of osseointegration, which was defined as direct structural and functional connection between ordered living bone and the surface of a load-carrying implant.<sup>11</sup> In clinical practice, roughened surfaces have been used to increase the total surface area available for osseous apposition.<sup>12,13</sup> However, the bioinert titanium material formed a biomechanical bonding rather than biochemical bonding with bony tissue. The mechanical interlocking required a period of relative immobilization. Failure to limit micromotion could cause loosening at the bone-implant interface.<sup>14-16</sup>

Bioceramic coatings and chemical treatment are 2 common methods used to create a bioactive tita-

niun surface. The coating most frequently utilized in clinical settings has been hydroxyapatite.<sup>17–20</sup> However, hydroxyapatite is usually degradable in body environments.<sup>21,22</sup>

Chemical treatment appears to be a simpler technique that can achieve a bioactive titanium surface. NaOH<sup>23–28</sup> and H<sub>2</sub>O<sub>2</sub><sup>29–32</sup> solutions were frequently employed in chemical treatment. NaOH treatment produces a sodium titanate gel layer on the titanium surface while H<sub>2</sub>O<sub>2</sub> treatment produces a titanium dioxide gel layer. Both layers can induce deposition of bonelike apatite during soaking in simulated body fluid. The materials bonded with bone through the apatite layer at an early implantation period. However, the bioactivity of the titanium dioxide gel originated from the favorable structure of the gel itself while the bioactivity of the sodium titanate gel depended heavily on ion release from the gel. Recently, it was reported that the treatment with H<sub>2</sub>O<sub>2</sub>/HCl solution at 80°C for 20 minutes followed by heating at 400°C for 1 hour formed a bioactive titanium dioxide gel layer that was able to induce rapid formation of apatite when soaked in simulated body fluid.<sup>31,32</sup> This indicated that the H<sub>2</sub>O<sub>2</sub>/HCl heat treatment had potential to improve bioactivity of titanium implants. However, it is unclear whether this treatment also improves new bone formation around implants in animal experiments.

New bioactive surfaces have been developed by using sandblasted, dual acid-etched, and H<sub>2</sub>O<sub>2</sub>/HCl heat treatments.<sup>33</sup> Roughened surfaces are achieved after sandblasting and dual acid-etched treatments. The samples are heat-treated with H<sub>2</sub>O<sub>2</sub>/HCl solution. Therefore, a bioactive titanium dioxide gel layer formed on the roughened surface. This surface incorporates the advantages of roughened surfaces and bioactivity. The objective of this study was to investigate bone formation on this new surface and the effect of H<sub>2</sub>O<sub>2</sub>/HCl heat treatment on peri-implant bone formation by *in vivo* examination.

## MATERIALS AND METHODS

### Design and Surface Treatment of Ti-6Al-4V Implants and Discs

A total of 20 custom-made, screw-shaped, Ti-6Al-4V implants and 30 Ti-6Al-4V discs of 10 × 10 × 1 mm<sup>3</sup> (Xihu Biomaterial Research Institute, Hangzhou, China) were used in this study. The implants were 3 mm in diameter and 10 mm in length. Ten implants and 15 discs were treated different ways.

- Treatment 1, sandblasted and dual acid-etched group (control group): Half the implants and discs

were polished; sandblasted with large grits (green silicon carbide) at a pressure of 4 MPa; and washed with acetone, 75% alcohol, and distilled water in an ultrasonic cleaner, respectively, for 15 minutes. Subsequently, the specimens were chemically treated with a solution containing 0.11 mol/L HF and 0.09 mol/L HNO<sub>3</sub> at room temperature for 10 minutes and dried at 50°C for 24 hours. Then, the specimens were treated with a solution containing 5.80 mol/L HCl and 8.96 mol/L H<sub>2</sub>SO<sub>4</sub> at 80°C for 30 minutes and dried at 50°C for 24 hours.

- Treatment 2, sandblasted, dual acid-etched, and H<sub>2</sub>O<sub>2</sub>/HCl heat-treated group (test group): The remaining discs and implants were treated in the same manner as previously described after which the implants were further treated with a solution containing 8.8 mol/L H<sub>2</sub>O<sub>2</sub> and 0.1 mol/L HCl at 80°C for 20 minutes, dried at 50°C for 24 hours, and heat-treated at 400°C for 1 hour.<sup>33</sup>

### Surface Analysis of the Discs

Surface morphology of the discs was observed by field-emission SEM (FSEM, FEI, SIRION100, Eindhoven, The Netherlands). Scanning electron micrographs were taken at several chosen areas on 10 discs of both groups. Surface roughness of the discs was performed by atomic force microscopy (AFM, SPA400, Seiko Instrument, Chiba, Japan), and the measuring area was 0.1 × 0.1 mm. Five samples of each group were performed. Ten areas of 1 sample were arbitrarily chosen. The roughness was measured by mean values. Two measurements, Sa and the maximum peak-to-valley ratio, were performed on each sample. Sa is the arithmetic mean of the absolute values of the surface departures from a mean plane within the sampling area.<sup>34</sup> The maximum peak-to-valley ratio is the maximum distance from peak to valley of the entire measurement area. The mean Sa and the maximum peak-to-valley ratio values were statistically analyzed. Crystal structure of ten surfaces was analyzed by low-angle X-ray diffractometry. Low-angle X-ray diffractometry patterns were recorded with a Rigaku RAD-II diffractometer using CuKα radiation operating under 40 kV and 25 mA acceleration at an angle of incidence of 1 degree.

### Animals and Surgical Procedure

Throughout this study, the rabbits used were treated according to the guidelines for animal care established by Zhejiang University. All surgery was performed under sterile conditions in a veterinary operating room. The surgical procedure used has been reported previously.<sup>35</sup> Twenty implants were inserted into the bilateral femurs of 10 adult white rabbits weighing between 2.5 and 3.0 kg. The animals



**Fig 1** Surgical placement of the implants.

were anesthetized by an intramuscular injection of SuMianXin II (0.1 to 0.2 mL/kg, Military Veterinary Institute, Quartermaster University of PLA, China) and local administration of 0.5% lidocaine. The distal aspect of the femur was surgically exposed by incisions through the skin, fascia, and periosteum. The distal femoral condyles were chosen as experimental sites. The test implant was placed in the right femur, and the control implant was placed in the left. Thus, every rabbit served itself as comparison. By drilling intermittently at a low rotary speed and profuse saline irrigation, 1 osteotomy was prepared and sequentially enlarged to 3 mm in diameter. The implants were inserted without tapping until the implant abutments were level with the bone surface (Fig 1). After implantation, the animals received antibiotics (penicillin, 400,000 U/d) for 3 days.

### Fluorescent Bone Labeling

Fluorescent labels were administered to monitor new bone formation. Oxytetracycline hydrochloride (FLUKA, 200 mg/mL, 20 mg/kg i.m.) was administered at 7 and 49 days after implantation. Calcein green (Shanghai Sangon Biological Engineering company, 25 mg/mL, 5 mg/kg i.m.) was administered at 35 days following implantation.

### Euthanasia and Histological Processing

Eight weeks following implantation, the animals were euthanized with an overdose of SuMianXin II (1.0 mL, i.m.). Block specimens, including the implants and surrounding tissues, were dissected from all animals. Specimens were stored in 10% neutral buffered formalin for 5 to 7 days. Undecalcified cut and ground sections were prepared with the EXAKT system.<sup>36</sup> Two sections were taken from the

central part of each specimen. Sections were cut to a thickness of 200  $\mu\text{m}$ . The sections were ground and polished to a final thickness of approximately 30  $\mu\text{m}$ . One section was analyzed for fluorescent light microscopy. One section was stained with Stevenel's blue and van Gieson's picro fuchsin for analysis of histological examination.

### Histological and Histometric Examination

Incandescent light microscopy (BX51, Olympus, Tokyo, Japan) was used to observe the histological behavior, including observations of peri-implant bone formation, woven and lamellar bone, fibrovascular tissue, and marrow.

Dynamic labeling of new bone formation was evaluated with fluorescent light microscopy (BX51TR-32FB3-E01, Olympus, Tokyo, Japan). Active bone formation was evaluated relative to the presence or absence, intensity, and width of the fluorochrome markers (evidenced by yellow or light green labels, respectively).

One experienced masked examiner performed the histometric analysis by using light microscopy and a PC-based image analysis system (Image-Pro Plus, Media Cybernetics, Silver Spring, Maryland, USA). The following measurements were recorded for both surfaces of each implant: bone-to-implant contact, bone-to-implant contact for 3 consecutive threads, bone area within all implant threads, bone area 500  $\mu\text{m}$  outside of implant threads, and bone area within 3 consecutive threads.

### Statistical Analysis

Group means and standard deviations were used to calculate each parameter. Differences between experimental samples were analyzed by using Student's paired *t* test. A *P* value < .05 was required for statistical significance. SPSS 12.0 (SPSS, Chicago, Illinois, USA) was used for all statistical analysis.

## RESULTS

### Surface Analysis of the Discs

Microscopic evaluation demonstrated no residual particles from sandblasting for either the test or control surfaces (Fig 2). The surfaces were quite irregular for both techniques, but the peroxide-treated test surface demonstrated consistently smaller surface irregularities.

The mean Sa values for the control and peroxide treated test discs were  $0.75 \pm 0.14 \mu\text{m}$  and  $1.06 \pm 0.12 \mu\text{m}$ . The differences in Sa values were significant (*P* = .022). The mean values of the maximum peak-to-valley ratio for the control and peroxide-treated test

**Fig 2** FSEM micrographs of the control (a and b) and test (c and d) discs. The surfaces were quite irregular for both techniques; however, the peroxide treated test surface demonstrated consistently smaller surface irregularities.

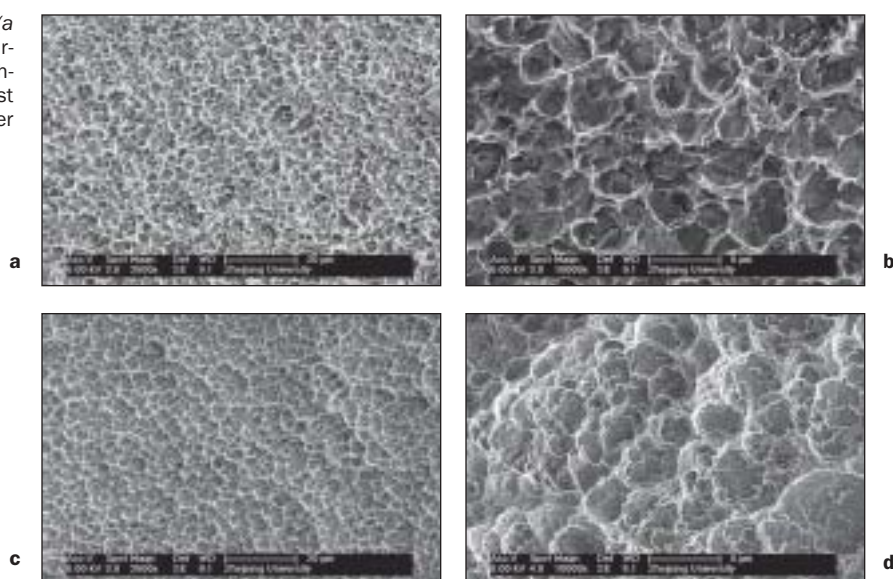
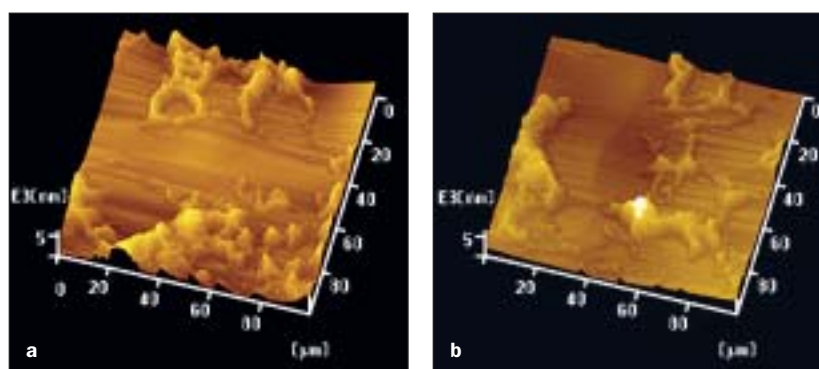


**Fig 3** AFM micrographs of the control (a) and test (b) discs



discs were  $0.64 \pm 0.04 \mu\text{m}$  and  $0.68 \pm 0.08 \mu\text{m}$ . No significant differences were found in the maximum peak-to-valley ratio values ( $P = .258$ ) (Fig 3).

Radiographic diffraction demonstrated a titanium dioxide layer on the surface of the peroxide-treated test implant. The crystal structure of titanium dioxide was anatase, the rarest form of titanium dioxide. However,  $\text{TiH}_2$  diffractions appeared on the X-ray diffractometry pattern of the control surface while  $\text{TiH}_2$  diffractions did not appear on the peroxide-treated test surface (Fig 4).

All animals appeared to be in good health throughout the test periods. At sacrifice, neither clinical signs of inflammation nor adverse tissue reaction were observed around the implants. All implants were in situ at sacrifice.

### Histological Observation

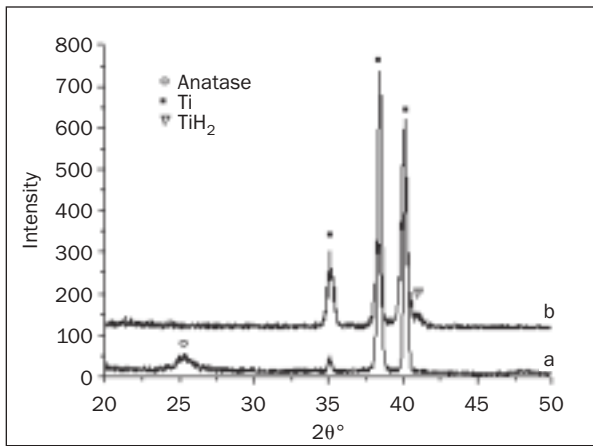
Incandescent light microscopy evaluation demonstrated new bone formation on the test and control implants. The bone-implant contact pattern

appeared to produce a broad-based direct contact (Fig 5). However, there were differences in the bone contact pattern. The contact of the test implants was more continuous and tighter than that of the control implants (Fig 6). The bone trabeculae in the vicinity of the implants was thin, the marrow cavity was large on the control implants, and intervening fibrous tissue was found along the interface. In the test group, the bone trabecular in the vicinity of the implants was thick and fibrous tissue along the implant surface was scarce.

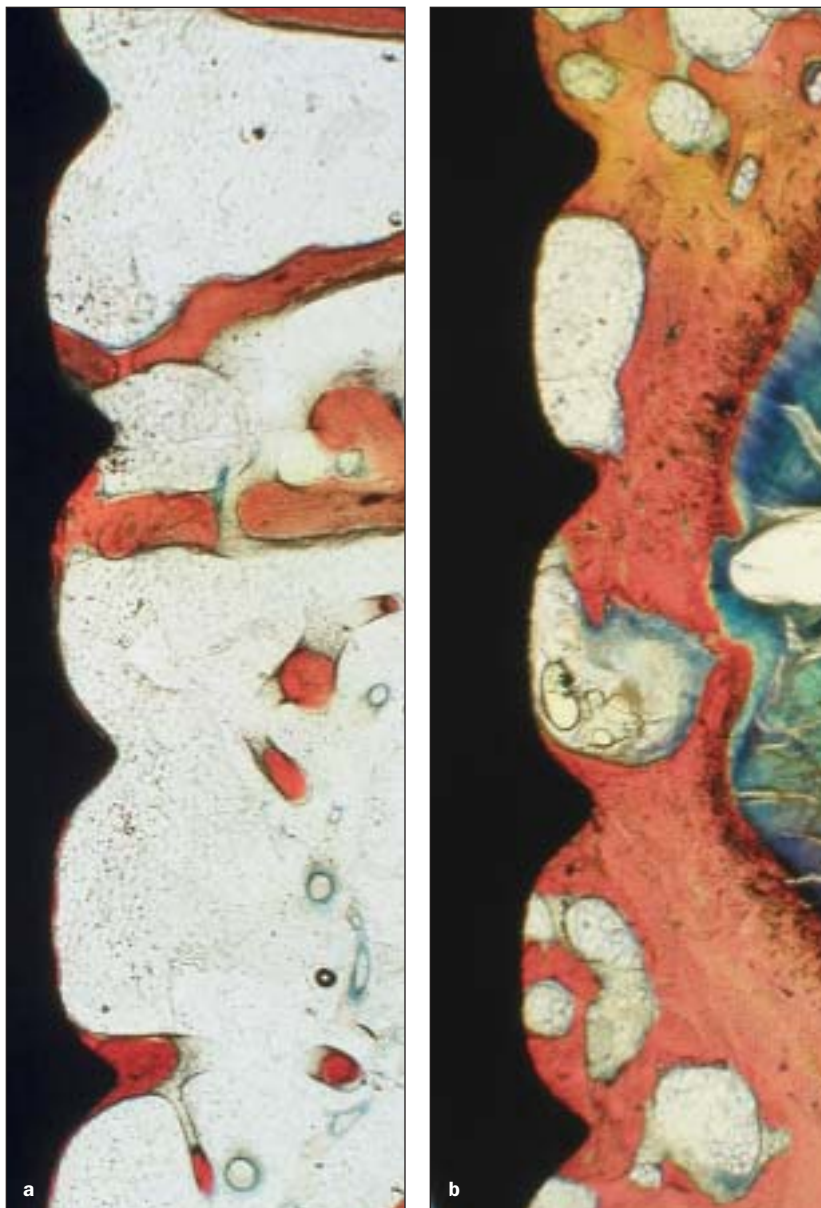
Fluorescence microscopy evaluation was similar to the incandescent light microscopy evaluation. The fluorescent bone labels demonstrated new bone formation on both implant surfaces. Yellow and light green were more evident in the test implant than in the control under the fluorescent light photomicrograph (Fig 7).

The bone-to-implant contact and bone area results from the histometric evaluation are presented in Figs 8 and 9. Test implants demonstrated 7.13%



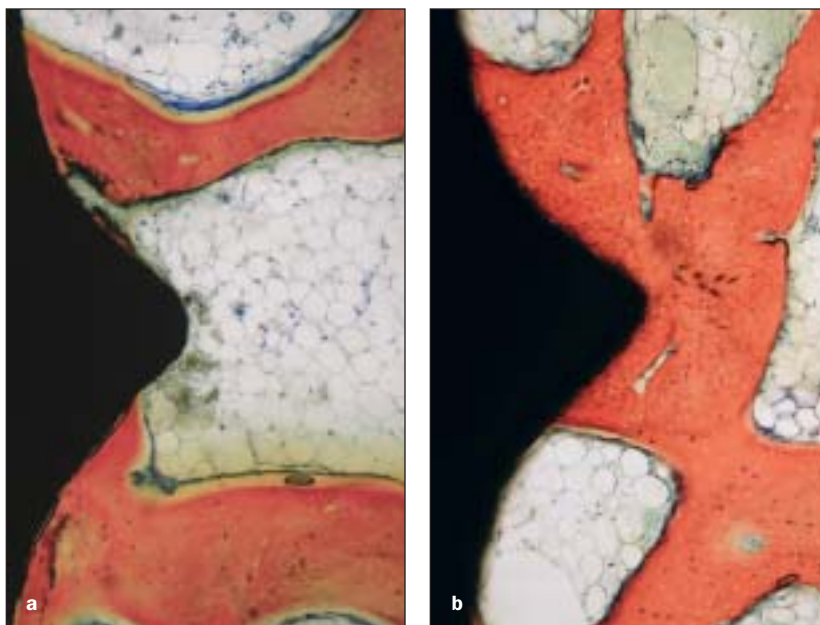


**Fig 4** XRD patterns of the test (a) and control (b) surfaces.

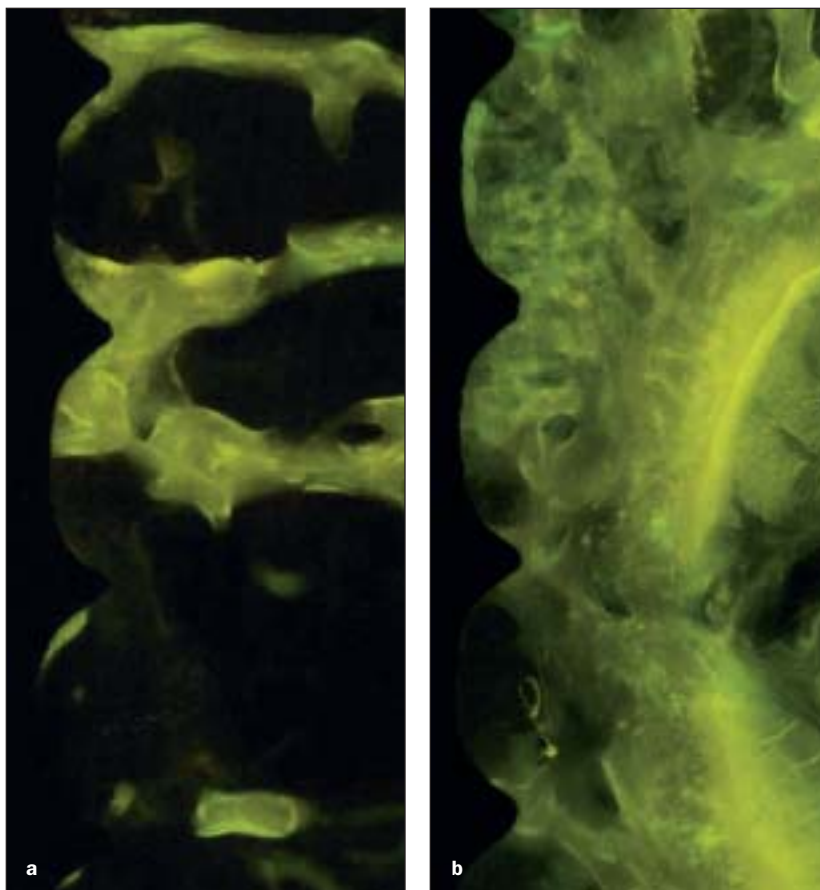


**Fig 5** Incandescent light photomicrographs of the control (a) and test (b) implants at low magnification. The bone-implant contact pattern appeared to produce a broad-based direct contact on both implant surfaces. The new bone formed on the test surface was more than that on the control surface.

**Fig 6** Incandescent light photomicrographs of the control (a) and test (b) implants at high magnification. The contact of the test implants was more continuous and tighter than that of the control implants. The bone trabeculae of the test implants was thicker than that of control implants.



**Fig 7** Fluorescent light photomicrographs of the control (a) and test (b) implants. The bone-implant contact on both groups was evident. In the test implant, yellow and light green were more evident than in the control.



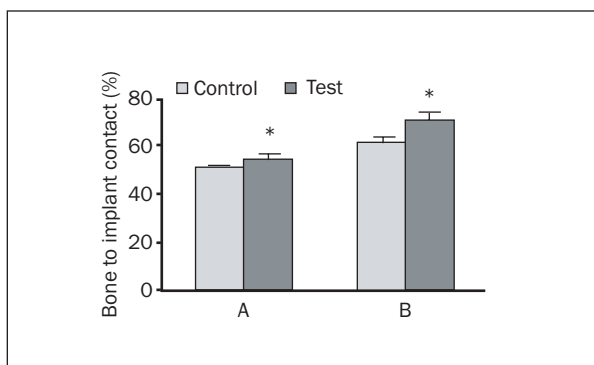


**Fig 8** Results of the histometric analysis of bone-to-implant contact for the control and test implant surfaces (mean  $\pm$  SD in %,  $N = 10$ ). a: bone-to-implant contact; b: bone-to-implant contact for 3 consecutive threads; asterisk,  $P < .05$ .

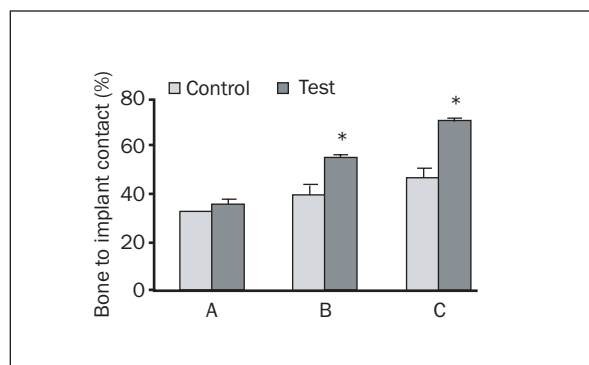


**Fig 9** Results of the histometric analysis of bone area for the control and test implant surfaces (mean  $\pm$  SD in %,  $n = 10$ ): a: bone area within all implant threads; b: bone area 500  $\mu\text{m}$  outside the implant threads; c: bone area within 3 consecutive threads; asterisk,  $P < .05$ .

more bone to implant contact ( $P = .003$ ) and 15.42% more bone to implant contact for 3 consecutive threads ( $P = .001$ ) than did control implants (Fig 8). Test implants demonstrated 37.04% more bone area, 500  $\mu\text{m}$  outside of implant threads ( $P = .004$ ), and 51.97% more bone area within 3 consecutive threads ( $P = .001$ ) than did control implants. No significant difference was found in bone area within all implant threads between the 2 groups ( $P = .069$ ) (Fig 9).

## DISCUSSION

It became apparent that bone-to-implant contact, bone area within 3 consecutive threads, and bone area outside of implant threads significantly increased in the peroxide-treated test group. This indicates that  $\text{H}_2\text{O}_2/\text{HCl}$  heat treatment of titanium implant can increase bone-to-implant contact and peri-implant bone formation. This phenomenon is similar to the results reported in some literature. Treatment of a commercial, machined surface titanium implant with  $\text{H}_2\text{SO}_4/\text{H}_2\text{O}_2$  solution enhanced significantly contact osteogenesis.<sup>37</sup> Kaneko approved the treatment with hydrogen peroxide solution containing tantalum chloride which provided higher bonding ability.<sup>38</sup> Detailed quantitative analysis of the bonding ability of an implant heat-treated with  $\text{H}_2\text{O}_2/\text{HCl}$  solution should be researched further.

Roughened surfaces on dental implants demonstrate cellular recruitment that results in earlier bone-to-implant contact.<sup>39–43</sup> Although the advantage of increased bone-to-implant contact has not demonstrated clinically significant improvements in implant survival,<sup>44,45</sup> rapid bone formation appears to be logically associated with improved clinical performance when endosseous implants are occlusally

loaded soon after placement. Studies on this topic have been underpowered and not demonstrated significant differences. In this study,  $\text{H}_2\text{O}_2/\text{HCl}$  heat treatment provided the test implant surfaces with smaller surface irregularities, bigger surface roughness, and a titanium-dioxide layer. Smaller surface irregularities can increase the interlocking capacity of implant surfaces and enable a favorable stress distribution of the functional loading of an implant at the interface. The peroxide-treated test implant surfaces belong to moderately rough surfaces ( $S_a$  between 1.0 and 2.0  $\mu\text{m}$ ), which show stronger bone responses than smoother or rougher surfaces.<sup>41</sup> The titanium dioxide layer can induce apatite deposition, which also favors bone formation. These support the differences in bone-to-implant contact and bone formation between the control and the test implants.

An essential requirement for the material to bond to living bone is the formation of a biologically active bonelike apatite layer on material surface in a body environment.<sup>46–48</sup> Titanium oxide hydrogel is 1 of the substances that induces apatite deposition on the surface. There are 3 crystal structures of titanium dioxide gels, including amorphous structure, anatase, and rutile.<sup>49</sup> Studies have shown that anatase and rutile can induce apatite deposition; anatase is better in depositing apatite than rutile.<sup>50–52</sup> In this study, anatase was formed on the peroxide-treated test implant surface, and there was  $\text{TiH}_2$  on the control implant surface. However,  $\text{TiH}_2$  did not play a significant role in bone response to the implant surface.<sup>53</sup>  $\text{H}_2\text{O}_2/\text{HCl}$  heat treatment can also provide apatite formation on titanium implant surface due to the formation of a large amount of  $\text{Ti-OH}$  groups. Thus, the obtained surface condition favors apatite formation. Observation and analysis of existence of the apatite layer in vivo is expected during further research.

The anatase gel coatings were traditionally derived by the sol-gel technique by hydrolysis of titanium alkoxides.<sup>54,55</sup> Those sol-gel-derived coatings can induce apatite apposition in simulated body fluid if the coating exceeds a certain thickness (about 200 nm) and experiences a subsequent heat treatment at a proper temperature range (400 to 550°C). A Ta-ion incorporated anatase gel was obtained by treatment of titanium metal with H<sub>2</sub>O<sub>2</sub>/TaCl<sub>5</sub> solution. After a subsequent heat treatment above 300°C, this gel transformed from amorphous to an anatase crystal structure and thus became bioactive enough to deposit apatite.<sup>30,56</sup> In the present study, H<sub>2</sub>O<sub>2</sub>/HCl heat treatment was used to form the anatase gel on the test implant surface. This treatment is much simpler than the sol-gel processing in which the reactions are difficult to control due to the fast kinetics of the alkoxides of transition metals. The H<sub>2</sub>O<sub>2</sub>/HCl solution is also simple and practical compared with the H<sub>2</sub>O<sub>2</sub>/TaCl<sub>5</sub> solution. Therefore, it may be concluded that the H<sub>2</sub>O<sub>2</sub>/HCl heat treatment is a superior technique over the traditional sol-gel coating technique and the H<sub>2</sub>O<sub>2</sub>/TaCl<sub>5</sub> heat treatment in producing bioactive titanium dioxide gel coatings on titanium surfaces.

Chemical treatment of titanium with H<sub>2</sub>O<sub>2</sub>/HCl solution is, therefore, a simple method that has potential to improve bone formation. This treatment has the advantage that it simply provides titanium implants with bone-formation ability. Namely, the surface of the treated titanium implant has the ability to deposit apatite by itself to give osteoconductivity.

## CONCLUSION

These data indicated that implants heat-treated with H<sub>2</sub>O<sub>2</sub>/HCl solution enhanced peri-implant bone formation and suggested H<sub>2</sub>O<sub>2</sub>/HCl heat treatment played an important role in bone formation.

## ACKNOWLEDGMENTS

We would like to thank Xihu Biomaterial Research Institute for delivering the experimental implants and discs. Financial support from the Key Scientific and Technological Project Fund of Zhejiang province (Grant no. 2005C23006, China) is gratefully acknowledged.

## REFERENCES

- Cochran DL, Buser D, ten Bruggenkate CM, et al. The use of reduced healing times on ITI implants with a sandblasted and acid-etched (SLA) surface: Early results from clinical trials on ITI SLA implants. *Clin Oral Implants Res* 2002;13:144–153.
- Bornstein MM, Lussi A, Schmid B, Belser UC, Buser D. Early loading of nonsubmerged titanium implants with a sandblasted and acid-etched (SLA) surface: 3-year results of a prospective study in partially edentulous patients. *Int J Oral Maxillofac Implants* 2003;18:659–666.
- Payne AG, Tawse-Smith A, Duncan WD, Kumara R. Conventional and early loading of unsplinted ITI implants supporting mandibular overdentures. *Clin Oral Implants Res* 2002;13:603–609.
- Salvi GE, Gallini G, Lang NP. Early loading (2 or 6 weeks) of sandblasted and acid-etched (SLA) ITI implants in the posterior mandible. A 1-year randomized controlled clinical trial. *Clin Oral Implants Res* 2004;15:142–149.
- Buser D, Mericske-Stern R, Bernard JP, et al. Long-term evaluation of nonsubmerged ITI implants. Part 1: 8-year life table analysis of a prospective multi-center study with 2359 implants. *Clin Oral Implants Res* 1997;8:161–172.
- Naert I, Koutsikakis G, Duyck J, Quirynen M, Jacobs R, van Steenberghe D. Biologic outcome of implant-supported restorations in the treatment of partial edentulism. part I: a longitudinal clinical evaluation. *Clin Oral Implants Res* 2002;13:381–389.
- Davarpanah M, Martinez H, Etienne D, et al. A prospective multicenter evaluation of 1,583 3i implants: 1- to 5-year data. *Int J Oral Maxillofac Implants* 2002;17:820–828.
- Sullivan DY, Sherwood RL, Porter SS. Long-term performance of Osseotite implants: a 6-year clinical follow-up. *Compend Contin Educ Dent* 2001;22:326–328, 330,332334.
- Friberg B, Gr;154;ndahl K, Lekholm U, Brånemark PI. Long-term follow-up of severely atrophic edentulous mandibles reconstructed with short Brånemark implants. *Clin Implant Dent Relat Res* 2000;2:184–189.
- Bahat O. Brånemark system implants in the posterior maxilla: Clinical study of 660 implants followed for 5 to 12 years. *Int J Oral Maxillofac Implants* 2000;15:646–653.
- Brånemark PI. Introduction to osseointegration. In: Brånemark PI, Zarb G, Albrektsson T (eds). *Tissue-Integration Prosthesis. Osseointegration in Clinical Dentistry*. Chicago: Quintessence, 1985:11–76.
- Cochran DL. A comparison of endosseous dental implant surfaces. *J Periodontol* 1999;70:1523–1539.
- Cochran DL, Buser D. Bone Response to sandblasted and acid-attacked titanium: experimental and clinical studies. In: Davies JE (ed). *Bone Engineering*. Toronto, Canada: Em Squared Inc, 2000:391–397.
- Buser D, Nydegger T, Oxland T, et al. Interface shear strength of titanium implants with a sandblasted and acid-etched surface: A biomechanical study in the maxilla of miniature pigs. *J Biomed Mater Res* 1999;45:75–83.
- Li D, Ferguson SJ, Beutler T, et al. Biomechanical comparison of the sandblasted and acid-etched and the machined and acid-etched titanium surface for dental implants. *J Biomed Mater Res* 2002;60: 325–332.
- Perrin D, Szmukler-Moncler S, Echikou C, Pointaire P, Bernard JP. Bone response to alteration of surface topography and surface composition of sandblasted and acid-etched (SLA) implants. *Clin Oral Implants Res* 2002;13:465–469.
- Wang H, Eliaz N, Xiang Z, Hsu HP, Spector M, Hobbs LW. Early bone apposition in vivo on plasma-sprayed and electrochemically deposited hydroxyapatite coatings on titanium alloy. *Biomaterials* 2006;27:4192–4203.
- Schopper C, Moser D, Goriwoda W, et al. The effect of three different calcium phosphate implant coatings on bone deposition and coating resorption: A long-term histological study in sheep. *Clin Oral Implants Res* 2005;16:357–368.



19. Ferro D, Barinov SM, Rau JV, Teghil R, Latini A. Calcium phosphate and fluorinated calcium phosphate coatings on titanium deposited by Nd:YAG laser at a high fluence. *Biomaterials* 2005;26:805–812.
20. Yildirim OS, Aksakal B, Hanyaloglu SC, Erdogan F, Okur A. Hydroxyapatite dip coated and uncoated titanium poly-axial pedicle screws: An in vivo bovine model. *Spine* 2006;31:E215–E220.
21. Sennerby L, Thomsen P, Ericson LE. Ultrastructure of the bone–titanium interface in rabbits. *J Mater Sci Mater Med* 1992;3:262–271.
22. Klein CPAT, Wolke JGC, de Groot K. Stability of calcium phosphate ceramics and plasma sprayed coating. In: Hench LL, Wilson J (eds). *An Introduction to Bioceramics*. Singapore: World Science, 1993:199–222.
23. Kokubo T, Miyaji F, Kim HM, Nakamura T. Spontaneous formation of bone-like apatite layer on chemically treated titanium metals. *J Am Ceram Soc* 1996;79:1127–1129.
24. Kim HM, Miyaji F, Kokubo T, Nakamura T. Preparation of bioactive Ti and its alloys via simple chemical surface treatment. *J Biomed Mater Res* 1996;32:409–417.
25. Kim HM, Miyaji F, Kokubo T, Nakamura T. Effect of heat treatment on apatite-forming ability of Ti metal induced by alkali treatment. *J Mater Sci Mater Med* 1997;8:341–347.
26. Wen HB, de Wijn JR, Cui FZ, de Groot K. Preparation of bioactive Ti6Al4V surfaces by a simple method. *Biomaterials* 1998;19:215–221.
27. Wen HB, Liu Q, de Wijn JR, de Groot K. Preparation of bioactive microporous titanium surface by a new two-step chemical treatment. *J Mater Sci Mater Med* 1998;9:121–128.
28. Ha SW, Eckert KL, Wintermantel E, Gruner H, Guecheva M, Vonmont H. NaOH treatment of vacuum-plasma-sprayed titanium on carbon fibre-reinforced poly (etheretherketone). *J Mater Sci Mater Med* 1997;8:881–886.
29. Ohtsuki C, Iida H, Hayakawa S, Osaka A. Bioactivity of titanium treated with hydrogen peroxide solution containing metal chlorides. *J Biomed Mater Res* 1997;35:39–47.
30. Wang XX, Hayakawa S, Tsuru K, Osaka A. Improvement of the bioactivity of H<sub>2</sub>O<sub>2</sub>/TaCl<sub>5</sub>-treated titanium after a subsequent heat treatment. *J Biomed Mater Res* 2000;52:171–176.
31. Wang XX, Hayakawa S, Tsuru K, Osaka A. A comparative study of in vitro apatite apposition on heat-, H<sub>2</sub>O(2)-, and NaOH-treated titanium surfaces. *J Biomed Mater Res* 2001;54:172–178.
32. Wang XX, Hayakawa S, Tsuru K, Osaka A. Bioactive titania-gel layers formed by chemical treatment of Ti substrate with a H<sub>2</sub>O<sub>2</sub>/HCl solution. *Biomaterials* 2002;23:1353–1357.
33. He FM, Zhao SS, Liu L, Chen S, Shen ZL, Wang XX. The preparation of the multilevel holes and analysis of the pure titanium surface. *Shanghai Kou Qiang Yi Xue* 2005;14:639–644.
34. Wennerberg A, Albrektsson T, Lausmaa J. Torque and histomorphometric evaluation of c.p. titanium screws blasted with 25- and 75-microns-sized particles Al<sub>2</sub>O<sub>3</sub>. *J Biomed Mater Res* 1996;30:251–260.
35. Nkenke E, Kloss F, Wiltfang J, et al. Histomorphometric and fluorescence microscopic analysis of bone remodeling after installation of implants using an osteotome technique. *Clin Oral Implants Res* 2002;13:595–602.
36. Donath K, Breuner G. A method for the study of undecalcified bones and teeth with attached soft tissues. The Säge-Schliff (sawing and grinding) technique. *J Oral Pathol* 1982;11:318–326.
37. Tavares MG, de Oliveira PT, Nanci A, Hawthorne AC, Rosa AL, Xavier SP. Treatment of a commercial, machined surface titanium implant with H<sub>2</sub>SO<sub>4</sub>/H<sub>2</sub>O<sub>2</sub> enhances contact osteogenesis. *Clin Oral Implants Res* 2007;18:452–458.
38. Kaneko S, Tsuru K, Hayakawa S, et al. In vivo evaluation of bone-bonding of titanium metal chemically treated with a hydrogen peroxide solution containing tantalum chloride. *Biomaterials* 2001;22:875–881.
39. Deporter DA, Watson PA, Pilliar RM, et al. A histological assessment of the initial healing response adjacent to porous-surfaced, titanium alloy dental implants in dogs. *J Dent Res* 1986;65:1064–1070.
40. Pilliar RM. Porous surfaced endosseous dental implants: fixation by bone ingrowth. *Univ Tor Dent J* 1988;1:10–15.
41. Albrektsson T, Wennerberg A. Oral implant surfaces: Part 1—review focusing on topographic and chemical properties of different surfaces and in vivo responses to them. *Int J Prosthodont* 2004;17:536–543.
42. Albrektsson T, Wennerberg A. Oral implant surfaces: Part 2—review focusing on clinical knowledge of different surfaces. *Int J Prosthodont* 2004;17:544–564.
43. Wennerberg A, Albrektsson T. Suggested guidelines for the topographic evaluation of implant surfaces. *Int J Oral Maxillofac Implants* 2000;15:331–344.
44. Eckert SE, Choi YG, Sánchez AR, Koka S. Comparison of dental implant systems: Quality of clinical evidence and prediction of 5-year survival. *Int J Oral Maxillofac Implants* 2005;20:406–415.
45. Esposito M, Coulthard P, Thomsen P, Worthington HV. The role of implant surface modifications, shape and material on the success of osseointegrated dental implants. A Cochrane systematic review. *Eur J Prosthodont Restor Dent* 2005;13:15–31.
46. Kokubo T. Bioactive glass ceramics: properties and applications. *Biomaterials* 1991;12:155–163.
47. Hench LL. Bioceramics. *J Am Ceram Soc* 1998;81:1705–1728.
48. Kokubo T, Kim HM, Kawashita M, Nakamura T. What kinds of materials exhibit bone-bonding ability. In Davies JE (ed). *Boneengineering*. Toronto, Canada: Em Squared, 2000:191–194.
49. Uchida M, Kim HM, Kokubo T, Fujibayashi S, Nakamura T. Structural dependence of apatite formation on titania gels in a simulated body fluid. *J Biomed Mater Res* 2003;64:164–170.
50. Miyata N, Fukea K, Chenb Q, Kawashita M, Kokubo T, Nakamura T. Apatite-forming ability and mechanical properties of PTMO modified CaO–SiO<sub>2</sub> hybrids prepared by sol–gel processing: Effect of CaO and PTMO contents. *Biomaterials* 2002;23:3033–3040.
51. Rohanizadeh R, Al-Sadeq M, LeGeros RZ. Preparation of different forms of titanium oxide on titanium surface: Effects on apatite deposition. *J Biomed Mater Res* 2004;71:343–352.
52. Wei M, Uchida M, Kim HM, Kokubo T, Nakamura T. Apatite-forming ability of CaO-containing titania. *Biomaterials* 2002;23:167–172.
53. Perrin D, Szmukler-Moncler S, Echikou C, Pointaire P, Bernard JP. Bone response to alteration of surface topography and surface composition of sandblasted and acid etched (SLA) implants. *Clin Oral Implants Res* 2002;13:465–469.
54. Peltola T, Patsi M, Rahiala H, Kangasniemi I, Yli-Urpo A. Calcium phosphate induction by sol–gel-derived titania coatings on titanium substrates in vitro. *J Biomed Mater Res* 1998;41:504–510.
55. Jokinen M, Patsi M, Rahiala H, Peltola T, Ritala M, Rosenholm JB. Influence of sol and surface properties on in vitro bioactivity of sol gel-derived TiO<sub>2</sub> and TiO<sub>2</sub>-SiO<sub>2</sub> films deposited by dipcoating method. *J Biomed Mater Res* 1998;42:295–302.
56. Ohtsuki C, Iida H, Hayakawa S, Osaka A. Bioactivity of titanium treated with hydrogen peroxide solution containing metal chlorides. *J Biomed Mater Res* 1997;35:39–47.
57. Wang XX, Hayakawa S, Tsuru K, Osaka A. Improvement of the bioactivity of H<sub>2</sub>O<sub>2</sub>/TaCl<sub>5</sub>-treated titanium after a subsequent heat treatment. *J Biomed Mater Res* 2000;52:171–176.

Copyright of *International Journal of Oral & Maxillofacial Implants* is the property of Quintessence Publishing Company Inc. and its content may not be copied or emailed to multiple sites or posted to a listserv without the copyright holder's express written permission. However, users may print, download, or email articles for individual use.